$(Pr_{0.7}Ca_{0.3})_{0.9}MnO_{3-\delta}$–SDC cathode for IT-SOFC

Lin Xiong [*], Shaorong Wang, Yuansong Wang, Ting-Lian Wen

Shanghai Institute of Ceramics, Chinese Academy of Sciences, Shanghai 200050, China

Abstract

$(Pr_{0.7}Ca_{0.3})_{0.9}MnO_{3-\delta}$ was synthesized by an EDTA–citrate complexing method. The powder was characterized with X-ray diffraction and transmission electron microscope. The thermal expansion curve and electrical conductivity of $(Pr_{0.7}Ca_{0.3})_{0.9}MnO_{3-\delta}$ was measured. Electrochemical properties of $(Pr_{0.7}Ca_{0.3})_{0.9}MnO_{3-\delta}$ cathode with and without SDC impregnation were studied by ac impedance analyzer. The results suggest that $(Pr_{0.7}Ca_{0.3})_{0.9}MnO_{3-\delta}$ impregnated with SDC is a suitable cathode for IT-SOFCs based on YSZ electrolyte.
© 2006 Elsevier B.V. All rights reserved.

Keywords: Fuel cells; Electrode materials; Sol–gel processes; Electronic properties; Thermal expansion

1. Introduction

Solid oxide fuel cells (SOFCs) are highly efficient and environment-friendly devices to generate electricity and heat. Conventional SOFCs work at as high a temperature as 1000 °C. In recent years, much effort has been made to reduce the SOFCs' operating temperature to 600–850 °C in order to reduce the cost and enhance the stability [1–3]. Although electrolytes such as $Ce_{1-x}Gd_xO_2$ (CGO) and $La_{0.9}Sr_{0.1}Ga_{0.8}Mg_{0.2}O_{2.85}$ (LSGM) show much higher ionic conductivity than yttrium-stabilized zirconia (YSZ), there are problems such as electronic conductivity in reducing atmospheres for CGO [4], and reactivity with electrodes for LSGM [5], which limit their application range or cells structure design. CGO is not suitable above 650 °C and LSGM has difficulty in preparing anode supported structure. Further more, there is still lack of stable supply of such electrolytes' powder, which is very important for cells manufacture engineering. Thus, zirconia-based electrolytes are still preferred in large SOFC stacks. In the newly developed anode supported cell structure, the electrolyte thickness is only 10–30 μm and many studies [6] have shown that the cathode polarization is the major contribution to the total resistance in such a cell. Therefore, more active cathode materials need to be developed for intermediate temperature SOFCs (IT-SOFCs) based on YSZ electrolyte.

Mixed ionic and electronic conducting oxides (MIEC) such as $(La,Sr)(Co,Fe)O_3$ (LSCF) [7] and $(Sm,Sr)CoO_3$ (SSC) [8] have shown high electrochemical activity for the O_2 reduction, but these cobaltite-based materials react easily with the YSZ electrolyte [9]. On the other hand manganite/electrolyte composites such as $(La,Sr)MnO_3$/YSZ [10] demonstrate both good performance and excellent compatibility. It has been reported that among various rare earth manganites, those incorporating Pr^{3+} exhibit the highest electrical conductivity and the lowest overpotential values [11]. And according to the report by Rim [12] Ca doped $PrMnO_3$ shows better performance than Sr doped $PrMnO_3$.

In the present work $(Pr_{0.7}Ca_{0.3})_{0.9}MnO_{3-\delta}$ is synthesized by a citrate–EDTA complexing method. The electrical conductivity and thermal expansion curve of $(Pr_{0.7}Ca_{0.3})_{0.9}MnO_{3-\delta}$ is measured. The electrochemical properties of pure $(Pr_{0.7}Ca_{0.3})_{0.9}MnO_{3-\delta}$ cathode and those impregnated with different loadings of Sm doped CeO_2 (SDC) are studied with ac impedance measurements.

2. Experimental

2.1. Powder synthesis and characterization

The $(Pr_{0.7}Ca_{0.3})_{0.9}MnO_{3-\delta}$ powder was prepared using a combined citrate and EDTA complexing method. Stoichiometric amounts of P_6O_{11}, $CaCO_3$, $MnCO_3$ (all in 99.9% purity) were dissolved in calculated amount of nitric acid. Then proper amounts of citric acid–H_2O solution and EDTA–NH_3·H_2O solution was added orderly while stirring. The mole ratio of EDTA acid:citric acid:total

---

* Corresponding author.
E-mail address: xionglin@mail.sic.ac.cn (L. Xiong).

metal ions was controlled to be around 1:1.5:1. Precipitation might occur after EDTA addition, $NH_3 \cdot H_2O$ was then added to adjust the pH value to around 6, and the solution become transparent immediately. EDTA–$NH_3 \cdot H_2O$ and citrate formed a buffering solution which keeps the pH value of the system around 6 during the whole process. With the evaporation of water, a dark yellow gel was obtained. The gel was then heated at 120 °C overnight to get the precursor, which was calcined at different temperatures for 5 h to obtain the powder of final composition.

TG/DTA analysis was carried out for the precursor in air from room temperature to 1200 °C with a heating rate of 10 °C/min. The powders calcined at 600 and 900 °C were subjected to X-ray diffraction (Rigaku XRD diffractometer) at room temperature. The morphology of powder was observed with a transmission electron microscope (JEM2010).

2.2. Measurements of thermal expansion behavior and electrical conductivity

The powder calcined at 900 °C was pressed uniaxially under 200 MPa into a rod compact with the length of 32 mm. Then the compact was sintered in air at 1350 °C for 10 h. For comparison, an additional YSZ compact was prepared and sintered at 1450 °C for 4 h. The sintered samples were used for thermal expansion and electrical conductivity measurements. Thermal expansion behavior was measured with a dilatometer, NETZSCH DIL 402PC. Electrical conductivity was measured by the four-probe dc technique, using Pt as electrodes. The relative density of the sintered sample was calculated from the sample weight, volume and lattice constants.

2.3. Measurement of cathode polarization

YSZ pellets of about 200 μm thick and 15 mm × 15 mm in area were used as electrolyte. The polarization resistance was measured by two-electrode impedance method using symmetric $(Pr_{0.7}Ca_{0.3})_{0.9}MnO_{3-\delta}$|YSZ|-$(Pr_{0.7}Ca_{0.3})_{0.9}MnO_{3-\delta}$ cells. $(Pr_{0.7}Ca_{0.3})_{0.9}MnO_{3-\delta}$ cathodes were screen printed on the YSZ pellets on both sides and then fired at 1000–1200 °C for 3 h. The cathode area is about 1 cm^2. The SDC impregnation was carried out by dropping $Sm_{0.2}Ce_{0.8}(NO_3)_x$ solution on top of the as fired $(Pr_{0.7}Ca_{0.3})_{0.9}MnO_{3-\delta}$ cathode surface, which was infiltrated by the solution through capillary effect. Then the sample was heat treated at 850 °C for 1 h to form the SDC phase. The impregnated SDC loading was controlled by changing the concentration of the $Sm_{0.2}Ce_{0.8}(NO_3)_x$ solution. For impregnated samples, each was weighed before screen-printing, after cathode firing and after SDC heat treatment. So the exact mass ratio of $(Pr_{0.7}Ca_{0.3})_{0.9}MnO_{3-\delta}$ to SDC can be determined. The polarization resistances were measured using an electrochemical workstation (Zahner IM6e). The impedance spectras of the cells were recorded at open circuit voltage (OCV) with amplitude of 10 mV over the frequency range of 0.1 Hz to 100 kHz.

3. Results and discussion

3.1. Powder characterization

Fig. 1 shows the TG/DTA curves for the precursor gel dried at 120 °C. The weight loss of nearly 80% occurred in the temperature range of 200–450 °C. The exothermic peaks in this temperature range may be attributed to the combustion in air of the polyester. Above 450 °C neither obvious weight change nor endothermic/exothermic peaks were observed, indicating that the peroskite phase may have formed at a temperature as low as 500 °C.

Fig. 2 shows the XRD patterns of the powders calcined at different temperatures. It is clear that the powder calcined at 600 °C has formed the peroskite phase, which conforms to the TG/DTA result. The peaks of the powder calcined at lower temperature are
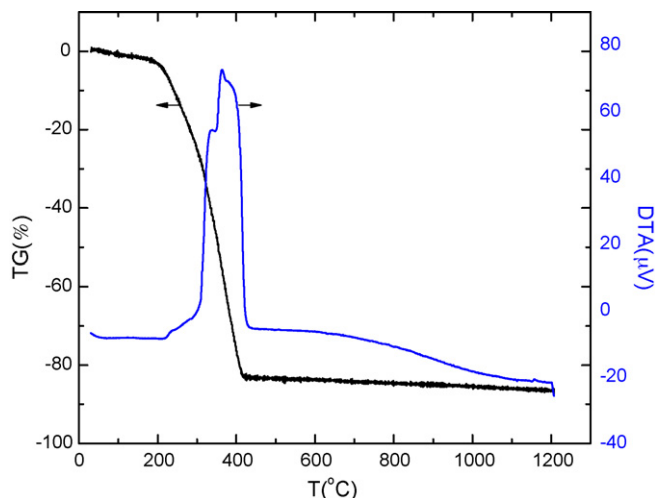

Fig. 1. TG/DTA curves for the dried precursor.

much broader than that of the powder calcined at higher temperature, indicating much smaller particle size of the powder calcined at lower temperature. Through computation using a least squares refinement the $(Pr_{0.7}Ca_{0.3})_{0.9}MnO_{3-\delta}$ was found to have an orthorhombic structure. The lattice parameters are $a = 5.416$ Å, $b = 5.430$ Å, $c = 7.664$ Å, and theoretic densities is 5.97 g/cm^3.

Fig. 3 shows the transmission electron microscope image of the powders calcined at 600 and 900 °C. It can bee seen that the powder calcined at 600 °C has an average particle size of about 50 nm while the powder calcined at 900 °C shows an average particle size of larger than 200 nm and more severe agglomeration.

3.2. Thermal expansion behavior and electrical conductivity

Fig. 4 shows the thermal expansion curves of $(Pr_{0.7}Ca_{0.3})_{0.9}MnO_{3-\delta}$ and YSZ in air. The curve of $(Pr_{0.7}Ca_{0.3})_{0.9}MnO_{3-\delta}$ is
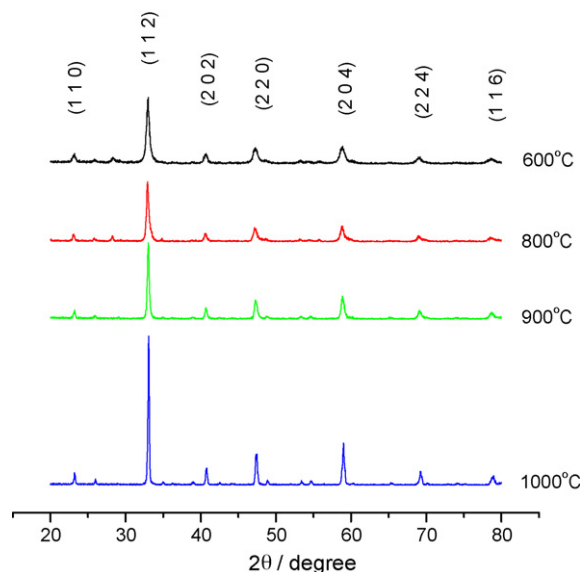

Fig. 2. XRD patterns of the peroskite powder calcined at different temperatures.
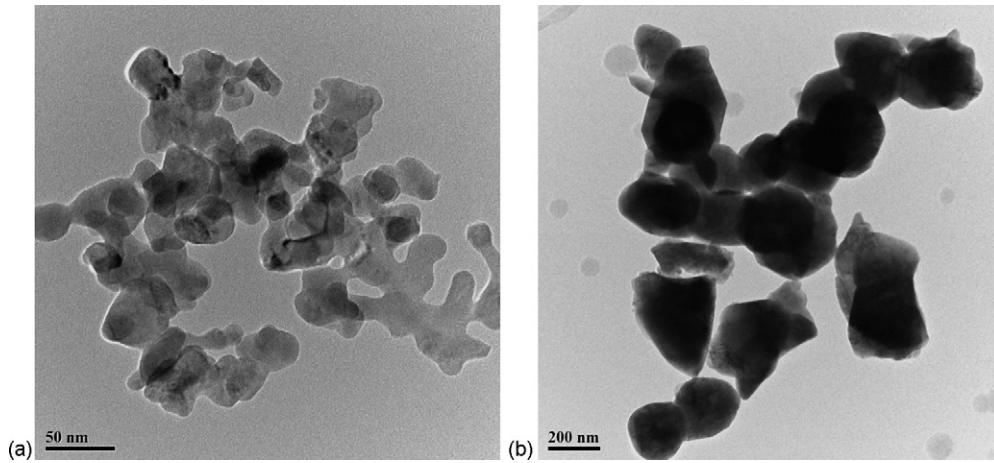
Fig. 3. TEM image for powders calcined at 600 °C (a) and 900 °C (b).

almost linear, but at elevated temperature above 750 °C, a slight increase in the slope can be observed. This may be attributed to the loss of lattice oxygen and formation of oxide ion vacancies [13]. Further calculation shows the average thermal expansion coefficient (TEC) between 25 and 1000 °C is $11.09 \times 10^{-6}\,\text{K}^{-1}$, very close to that of YSZ, $10.8030 \times 10^{-6}\,\text{K}^{-1}$. The small mismatch in TEC between $(Pr_{0.7}Ca_{0.3})_{0.9}MnO_{3-\delta}$ and YSZ can be beneficial for the SOFC system in maintaining long term stability and enduring thermal cycle.

Fig. 5 shows the temperature dependence of the electrical conductivity of $(Pr_{0.7}Ca_{0.3})_{0.9}MnO_{3-\delta}$. The plot of $\log(\sigma T)$ versus $1/T$ is almost linear, which is consistent with the small polaron conduction mechanism [14]:

$$\sigma = \frac{C}{T} \exp\left(-\frac{E_a}{k_B T}\right)$$

where E_a is the activation energy; k_B the Boltzmann constant; T is the absolute temperature. Above 800 °C, the conductivity of $(Pr_{0.7}Ca_{0.3})_{0.9}MnO_{3-\delta}$ is higher than $150\,\text{S}\,\text{cm}^{-1}$, which is sufficient for the cathode of SOFC. It must be
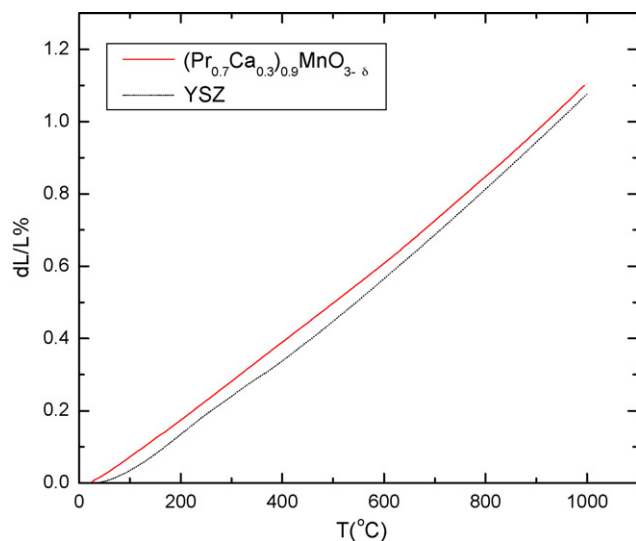
noted that the relative density of the sample measured here is about 92%.

3.3. Polarization resistance

Firing temperature is a critical parameter for a cathode to obtain good adhesion to electrolyte, suitable porosity and sufficient three-phase boundary (TPB) where the reduction of O_2 can occur. Fig. 6 gives the area specific resistances (ASR) measured at 800 °C for pure $(Pr_{0.7}Ca_{0.3})_{0.9}MnO_{3-\delta}$ cathode sintered at various temperatures. For powders calcined at 600 and 900 °C there is different optimal sintering temperatures. This can be explained because at lower sintering temperature the cathode cannot get a good adhesion with the electrolyte while at higher sintering temperature TPB becomes shorter due to the growth of cathode particles and the reduction in porosity. Besides, at sintering temperature of 1200 °C or above, zirconate phase easily forms between $(Pr_{0.7}Ca_{0.3})_{0.9}MnO_{3-\delta}$ and YSZ [15], which

Fig. 4. Thermal expansion curves of $(Pr_{0.7}Ca_{0.3})_{0.9}MnO_{3-\delta}$ and YSZ in air.
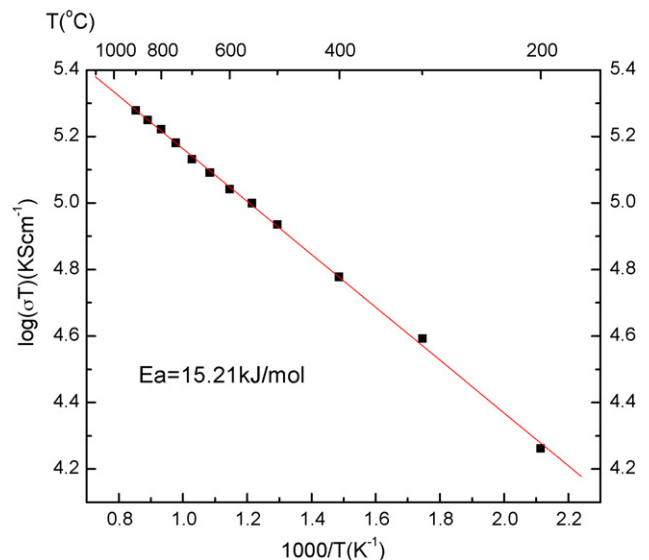

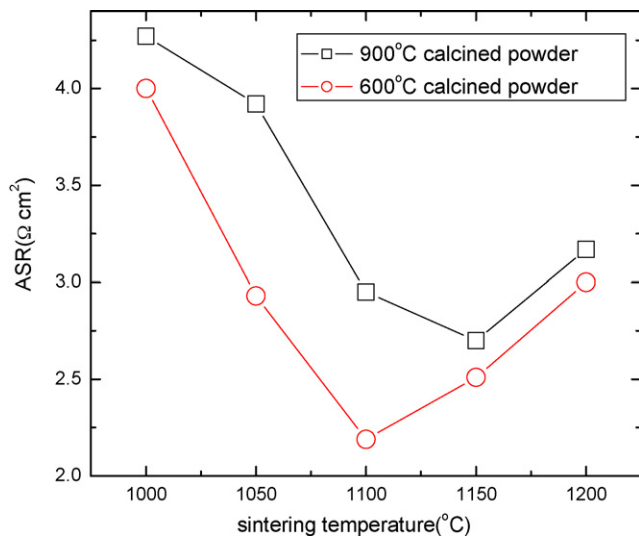Fig. 5. Electrical conductivity of $(Pr_{0.7}Ca_{0.3})_{0.9}MnO_{3-\delta}$ between 200 and 900 °C.

Fig. 6. Area specific resistance of pure $(Pr_{0.7}Ca_{0.3})_{0.9}MnO_{3-\delta}$ cathodes sintered at various temperatures, measured at 800 °C in air.

Fig. 7. Arrhenius plot of area specific resistance for $(Pr_{0.7}Ca_{0.3})_{0.9}MnO_{3-\delta}$ cathode impregnated with different SDC loadings.

can also lead to substantial increase in cathode polarization resistance. In fact, delamination was more or less observed for cathodes sintered below 1100 °C after testing. However it is still interesting to find that the cathodes made from the powder calcined at 600 °C generally shows lower polarization resistance than those made from the powder calcined at 900 °C. And the optimal sintering temperature for the powder calcined at 600 °C is lower than that for the powder calcined at 900 °C. This may be due to the smaller particle size and better sintering ability of the powder calcined at low temperature. This result suggests that the fabrication process plays an important role in determining the final cathode performance.

Because the cathode made from the 600 °C calcined powder and sintered at 1100 °C shows the lowest ASR, further SDC impregnation investigation was carried out on $(Pr_{0.7}Ca_{0.3})_{0.9}MnO_{3-\delta}$ cathode prepared at the same calcining and sintering temperatures. Four samples were prepared for SDC impregnation, with the SDC wt.% to be 0 (sample A), 13.51 (sample B), 21.93 (sample C), and 28.4 (sample D), respectively. The sample A was not impregnated.

Fig. 7 shows the Arrhenius plot of the area specific resistance for the four samples. It is obvious that as the SDC wt.% increases, the polarization resistance becomes smaller. At 850 °C the ASR of sample A, without impregnation, is 1 Ω cm^2, while the ASR of sample D, with 28.4 wt.% SDC is only about 0.29 Ω cm^2. However the activation energy values on the four samples are close (all in the range of 155 ± 10 kJ/mol), which is in agreement with Jiang's result [16] on the (La,Sr)MnO$_3$(LSM) cathode impregnated with CGO. This indicates that the SDC impregnation may not change the rate-limiting mechanism for the cathode reaction process. The reduction in polarization resistance is more likely to be caused by the increase in the TPB area. It is known that SDC has a high oxide ion conductivity, ~0.1 S cm^{-1} at 800 °C [17]. As the SDC loading increases, the deposited nano-sized SDC particles gradually form a continuous ionic conducting path, extending the reaction sites from the electrode/electrolyte interface to the bulk of the cathode. In Jiang's report [16], the
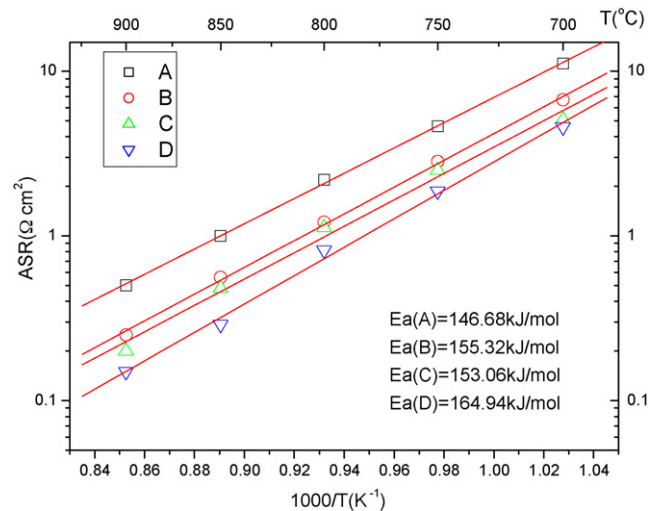
ASR of the impregnated LSM cathode is about 1/56 of that of the pure LSM cathode under 200 mA/cm^2 current at 700 °C. In our experiment, however, the reduction of ASR by impregnation was less obvious, although the ASR of the sample D is less than half of that of sample A at various temperatures. Except difference in materials and measuring conditions, the amount of impregnated phase may be an important reason for this. In Jiang's report the lowest ASR was achieved with a CGO loading of 5.8 mg/cm^2, but in this work the SDC loading of sample D is only 2.3 mg/cm^2 and less than 30 wt.% of the final cathode. In fact, in our experiment it seems difficult to impregnate more SDC without forming a separate SDC layer on the cathode surface. So if the porosity of the pure $(Pr_{0.7}Ca_{0.3})_{0.9}MnO_{3-\delta}$ cathode can be increased, the ASR may be further reduced by impregnation.

4. Conclusions

Single phase $(Pr_{0.7}Ca_{0.3})_{0.9}MnO_{3-\delta}$ was synthesized by a combined EDTA–citrate complexing method at 600 °C. The as-synthesized powder shows an orthorhombic structure at room temperature and an average particle size of about 50 nm. The average thermal expansion coefficient of $(Pr_{0.7}Ca_{0.3})_{0.9}MnO_{3-\delta}$ between 25 and 1000 °C is very close to that of YSZ. The electrical conductivity of $(Pr_{0.7}Ca_{0.3})_{0.9}MnO_{3-\delta}$ is higher than 150 S cm^{-1} above 800 °C. Low synthesizing temperature leads to nano-sized powder and better electrochemical performance of the obtained cathode. The SDC impregnation reduced the ASR of $(Pr_{0.7}Ca_{0.3})_{0.9}MnO_{3-\delta}$ cathode to less than a half. $(Pr_{0.7}Ca_{0.3})_{0.9}MnO_{3-\delta}$ cathode impregnated with 28.4 w.t.% SDC shows an ASR of 0.29 Ω cm^2 at 850 °C. The results suggest that $(Pr_{0.7}Ca_{0.3})_{0.9}MnO_{3-\delta}$ cathode impregnated with SDC is suitable for IT-SOFCs based on YSZ electrolyte.

References

[1] S.C. Singhal, Solid State Ionics 135 (2000) 305.
[2] J.M. Ralph, A.C. Schoeler, M. Krumpelt, J. Mater. Sci. 36 (2001) 1161.

[3] B.C.H. Steele, Nature 414 (2001) 345.
[4] B.C.H. Steele, Solid State Ionics 129 (1997) 95.
[5] K. Huang, M. Feng, J. Goodenough, J. Am. Ceram. Soc. 79 (1996) 4.
[6] N.Q. Minh, J. Am. Ceram. Soc. 76 (1993) 563.
[7] S. Wang, Torhrukato, S. Nagata, Solid State Ionics 146 (2002) 203.
[8] M. Koyama, C.-J. Wen, et al., J. Electrochem. Soc. 148 (2001) 795.
[9] H. Uchida, S.-I. Arisaka, M. Watanabe, Electrochem. Solid-State Lett. 2 (1999) 428.

[10] T. Tsai, S.A. Barnett, Solid State Ionics 93 (1997) 207.
[11] T. Ishihara, T. Kudo, et al., J. Electrochem. Soc. 142 (1995) 1519.
[12] H.R. Rim, S.K. Jeung, et al., Mater. Chem. Phys. 52 (1998) 54.
[13] L.-W. Tai, M.M. Nasrallah, et al., Solid State Ionics 76 (1995) 259.
[14] D. Pkarim, A.T. Aldred, Phys. Rev. B 20 (1979) 2255.
[15] J.P. Zhang, et al., J. Mater. Chem. 8 (1998) 2787.
[16] S.P. Jiang, W. Wang, Solid State Ionics 176 (2005) 1351.
[17] K. Eguchi, J. Alloys Compd. 250 (1997) 486.